

Motion of solitons in one-dimensional spin-orbit-coupled Bose-Einstein condensates

Lin Wen,^{1,2} Q. Sun,^{2,*} Yu Chen,² Deng-Shan Wang,³ J. Hu,² H. Chen,⁴ W.-M. Liu,⁴ G. Juzeliūnas,⁵
Boris A. Malomed,^{6,7} and An-Chun Ji^{2,†}

¹College of Physics and Electronic Engineering, Chongqing Normal University, Chongqing 401331, China

²Department of Physics, Capital Normal University, Beijing 100048, China

³School of Applied Science, Beijing Information Science and Technology University, Beijing 100192, China

⁴Institute of Physics, Chinese Academy of Sciences, Beijing 100190, China

⁵Institute of Theoretical Physics and Astronomy, Vilnius University, Saulėtekio Avenue 3, LT-10222 Vilnius, Lithuania

⁶Department of Physical Electronics, School of Electrical Engineering, Faculty of Engineering, Tel Aviv University, Tel Aviv 69978, Israel

⁷Laboratory of Nonlinear-Optical Informatics, ITMO University, St. Petersburg 197101, Russia

(Received 7 September 2016; published 8 December 2016)

Solitons play a fundamental role in the dynamics of nonlinear excitations. Here we explore the motion of solitons in one-dimensional Bose-Einstein condensates subjected to a spin-orbit coupling (SOC). We demonstrate that the spin dynamics of solitons is governed by a nonlinear Bloch equation. The spin dynamics affects the orbital motion of solitons leading to spin-orbit effects in the dynamics of macroscopic quantum objects (mean-field solitons). The latter perform oscillations with a frequency determined by the SOC, Raman coupling, and intrinsic nonlinearity. These findings reveal unique features of solitons affected by the SOC, which are confirmed by analytical considerations and numerical simulations of the underlying Gross-Pitaevskii equations.

DOI: [10.1103/PhysRevA.94.061602](https://doi.org/10.1103/PhysRevA.94.061602)

Solitons, which are generally realized as self-supported solitary waves, are among the most fundamental objects in nonlinear science. With the realization of Bose-Einstein condensates (BECs), matter-wave solitons have drawn enormous interest [1–9]. In experiments, both bright and dark solitons have been successively created in atomic BECs [1,10–14]. On the other hand, the successful realization of artificial spin-orbit coupling (SOC) in binary BECs [15–18] has stimulated intensive studies on novel SOC-induced effects [19–34]. In particular, a variety of solitons species, such as stripe modes, two-dimensional (2D) composite solitons, and half-vortex gap solitons, have been predicted in condensates combining the SOC, which is a linear interaction, and the intrinsic collisional nonlinearity [35–51]. In a ring-trapped BEC, Rashba SOC leads to the nontrivial magnetization dynamics of a dark soliton [52].

Soliton dynamics has been the subject of many studies carried out in various settings, including BEC [1–9], nonlinear optics [53–59], and others. In particular, it has been shown that harmonic trapping potentials induce the motion of solitons in quasi-one-dimensional (1D) BECs [60–65]. Due to the particlelike nature, the soliton dynamics differs essentially from the dipole mode of the noninteracting condensate loaded into the same potential. In particular, the oscillation frequency of trapped dark solitons differs by a factor $1/\sqrt{2}$ from the trap frequency [60]. Here, we address the soliton dynamics in 1D BECs under the action of Raman-induced SOC [15,16]. Since the Raman transition can flip the spin along with inducing a finite momentum transfer, the evolution of the spin degree of freedom may be coupled to the spatial motion of solitons. This effect, if it can be made conspicuous enough, may be considered as the SOC at the level of the motion

of a macroscopic quantum body, the matter-wave soliton. In this connection, it is relevant to mention a recent result showing that the SOC can induce anharmonic properties beyond the effective-mass approximation in collective dipole oscillations [16,66,67]. Yet the macroscopic SOC effects in the motion of solitons have yet to be explored, to the best of our knowledge.

In this Rapid Communication we investigate the soliton dynamics in 1D BEC influenced by the SOC. We find that an interplay of the SOC, Raman coupling, and nonlinearity induces precession of the soliton's spin \mathbf{S} under the action of an effective magnetic field, which is governed by a nonlinear Bloch equation (12). In turn, the spin precession couples to the orbital motion of the soliton via feedback onto its center-of-mass momentum, as shown below by the equation of motion (15) for the center-of-mass coordinate $\langle z \rangle$. Thus, Eqs. (12) and (15) directly demonstrate the effects of the SOC on the 1D motion of the macroscopic quantum object.

In the presence of SOC, the dynamics of the quasi-1D BECs, elongated in the direction of z , is modeled by the mean-field Gross-Pitaevskii (GP) equation,

$$i\partial_t \begin{pmatrix} \psi_\uparrow \\ \psi_\downarrow \end{pmatrix} = \hat{h}_0 \begin{pmatrix} \psi_\uparrow \\ \psi_\downarrow \end{pmatrix} + \begin{pmatrix} g_{\uparrow\uparrow}|\psi_\uparrow|^2, g_{\uparrow\downarrow}|\psi_\downarrow|^2 \\ g_{\downarrow\uparrow}|\psi_\uparrow|^2, g_{\downarrow\downarrow}|\psi_\downarrow|^2 \end{pmatrix} \begin{pmatrix} \psi_\uparrow \\ \psi_\downarrow \end{pmatrix}, \quad (1)$$

where ψ_σ are the pseudospin components of the BEC macroscopic wave function, with $\sigma = \uparrow, \downarrow$ labeling the spin states. These can represent, for instance, the hyperfine states $|1, -1\rangle$ and $|1, 0\rangle$ of ^{87}Rb atoms [15]. Here,

$$\hat{h}_0 = -\frac{1}{2}\partial_z^2 + V(z) + i\lambda\partial_z\sigma_z + \Omega\sigma_x + \delta\sigma_z \quad (2)$$

is a single-particle Hamiltonian which includes the Raman-induced SOC characterized by a strength λ , with Ω and δ describing, respectively, the frequencies of the Raman coupling and the Zeeman detuning. Here also $V(z) = \gamma^2 z^2/2$ is an effective 1D harmonic trap potential, and $\gamma \equiv \omega_z/\omega_\perp$ is the trap's aspect ratio, with ω_z and ω_\perp being the trapping

*QingSun@cnu.edu.cn

†anchun.ji@cnu.edu.cn

frequencies along the longitudinal and transverse directions, respectively. The frequencies and lengths are measured in units ω_{\perp} and $a_{\perp} = \sqrt{\hbar/m\omega_{\perp}}$, respectively, and, as mentioned above, $\lambda = k_L a_{\perp}$ represents the SOC strength, with k_L being the momentum transfer. Note that, as the strengths of the inter- and intraspecies atomic interactions are very close in the experiment, it is reasonable to assume SU(2)-symmetric spin interactions, with all components $g_{\sigma\sigma'}$ taking a single value g . To focus on the SOC effects on the dynamics of solitons, we first consider the free space, while the external trap will be discussed afterwards.

For $\lambda = \Omega = 0$, the system reduces to a normal binary BEC without the SOC. In this case, Eq. (1) is known as the integrable Manakov's system which gives rise to well-known exact soliton solutions [68]. In particular, bright-bright (BB) solitons are $\psi_{\sigma} = (\eta\epsilon_{\sigma}/\sqrt{-g})\text{sech}(\eta z)\exp(i\eta^2 t/2)$ for the attractive sign of the nonlinearity, $g < 0$, where η^{-1} is the soliton's width and ϵ_{σ} satisfies the normalized condition $|\epsilon_{\uparrow}|^2 + |\epsilon_{\downarrow}|^2 = -g/(2\eta)$. We use such exact soliton solutions as an initially prepared wave function, and then study the soliton dynamics as the SOC is switched on. Note that Eq. (2) is an effective single-particle Hamiltonian in the frame transformed via the local pseudospin rotation by angle $\vartheta = 2\lambda z$ about the z axis [15,16]. The transformation adds opposite phase factors $e^{\pm i\lambda z}$ to the two components of the input wave forms.

In the general case, the GP system (1) is no longer integrable. Therefore, we employ a variational approximation to investigate the soliton dynamics [5,69], based on the Lagrangian $L(t) = \int_{-\infty}^{+\infty} \{(i/2) \sum_{\sigma=\uparrow,\downarrow} [\psi_{\sigma}^*(\psi_{\sigma})_t - \psi_{\sigma}(\psi_{\sigma}^*)_t] - \mathcal{H}\} dz$, where \mathcal{H} is the Hamiltonian density of the system. We first consider the attractive nonlinearity, with $g < 0$. In this case, we introduce the following variational ansatz for BB solitons, with the total norm fixed to be 1,

$$\begin{pmatrix} \psi_{\uparrow} \\ \psi_{\downarrow} \end{pmatrix} = \sqrt{\frac{\eta}{2}} \begin{pmatrix} (\sin\theta)\text{sech}(\eta z + \xi_{\uparrow})e^{i(k_{\uparrow}z + \varphi_{\uparrow})} \\ (\cos\theta)\text{sech}(\eta z + \xi_{\downarrow})e^{i(k_{\downarrow}z + \varphi_{\downarrow})} \end{pmatrix}, \quad (3)$$

where $\theta, \eta, \xi_{\sigma}, k_{\sigma}, \varphi_{\sigma}$ are time-dependent variational parameters. Here, θ determines the population imbalance between the pseudospin components, η^{-1} defines their common width, k_{σ} is the wave number, and φ_{σ} the phase. For the SU(2) atomic interactions, two-component solitons favor the mixed phase [70]. Therefore, the positions of spin-up and spin-down solitons will overlap, $\xi_{\uparrow} = \xi_{\downarrow} = \xi$, as confirmed by the numerical simulations below.

Inserting the ansatz (3) into the Lagrangian and performing the integration, we obtain

$$\begin{aligned} L(t) = & \frac{\xi}{\eta} \frac{dk_{+}}{dt} - \frac{\xi}{\eta} \cos(2\theta) \frac{dk_{-}}{dt} - \frac{d\varphi_{+}}{dt} + \cos(2\theta) \frac{d\varphi_{-}}{dt} \\ & - \frac{1}{2} [k_{+}^2 - 2k_{+}k_{-} \cos(2\theta) + k_{-}^2] - \frac{1}{6} \eta^2 - \frac{1}{6} g \eta \\ & - \frac{\Omega \pi k_{-} \sin(2\theta) \cos(2\varphi_{-} - 2k_{-}\xi/\eta)}{\eta \sinh(\pi k_{-}/\eta)} \\ & + \delta \cos(2\theta) - \lambda [k_{+} \cos(2\theta) - k_{-}], \end{aligned} \quad (4)$$

where $k_{\pm} \equiv (1/2)(k_{\uparrow} \pm k_{\downarrow})$ and $\varphi_{\pm} \equiv (1/2)(\varphi_{\uparrow} \pm \varphi_{\downarrow})$. The evolution of the variational parameters is governed by the

corresponding Euler-Lagrangian (EL) equations (see the Supplemental Material [71] for details).

Note that the EL equations produce simple results, $\eta \approx -g/2$ and $k_{-} \approx \lambda$, in the case of a weak SOC, $\pi\lambda \ll \eta$. Indeed, in the absence of SOC, the relation $\eta = -g/2$ holds for the normalized wave function, indicating that the width of the solitons is determined by the nonlinearity, and k_{-} remains equal to the initial relative momentum λ between the components of the soliton. Thus, we arrive at a reduced system of the EL equations, in which η and k_{-} are considered as frozen quantities:

$$\dot{k}_{+} = 2\lambda\tilde{\Omega} \sin(2\theta) \sin\phi, \quad (5)$$

$$\dot{\phi} = -2\tilde{\Omega} \cot(2\theta) \cos\phi + 2\lambda k_{+} - 2\delta, \quad (6)$$

$$\dot{\theta} = -\tilde{\Omega} \sin\phi, \quad (7)$$

$$\dot{\langle z \rangle} = k_{+}. \quad (8)$$

Here, $\langle z \rangle = \int_{-\infty}^{+\infty} z(|\psi_{\uparrow}|^2 + |\psi_{\downarrow}|^2) dz \equiv -\xi/\eta$ is the center-of-mass coordinate, $\tilde{\Omega} = \Omega\pi\lambda/[\eta \sinh(\pi\lambda/\eta)]$, and $\phi \equiv 2\varphi_{-} + 2k_{-}\langle z \rangle$ is the phase difference between the two components of the soliton. Thus, Eqs. (5)–(8) account for the nonlinear coupling of the center-of-mass momentum k_{+} , phase difference ϕ , population imbalance θ , and center-of-mass coordinate $\langle z \rangle$.

We introduce a normalized complex-valued spinor $\chi = (\chi_{\uparrow}, \chi_{\downarrow})$ describing the two-component wave function $\psi_{\sigma} = \sqrt{\rho(z,t)}\chi_{\sigma}$, where $\rho \equiv |\psi_{\uparrow}|^2 + |\psi_{\downarrow}|^2$ is the total density, with $|\chi_{\uparrow}|^2 + |\chi_{\downarrow}|^2 = 1$. Furthermore, we define the spin density $S = \chi^T \sigma \chi$, where $\sigma \equiv \{\sigma_x, \sigma_y, \sigma_z\}$ is the vector set of the Pauli matrices. Therefore, we have $\{S_x, S_y, S_z\} = \{\sin(2\theta) \cos(2\lambda z + 2\varphi_{-}), -\sin(2\theta) \sin(2\lambda z + 2\varphi_{-}), -\cos(2\theta)\}$ for the ansatz given by Eq. (3). In this Rapid Communication, we focus on the center-of-mass motion of the soliton by setting $z = \langle z \rangle = -\xi/\eta$. Consequently, the evolution of the atomic spin at the soliton's center-of-mass is governed by the following equations,

$$\dot{S}_x = 2(\lambda c_1 - \delta) S_y - 2\lambda^2 S_z S_y, \quad (9)$$

$$\dot{S}_y = -2\tilde{\Omega} S_z - 2(\lambda c_1 - \delta) S_x + 2\lambda^2 S_z S_x, \quad (10)$$

$$\dot{S}_z = 2\tilde{\Omega} S_y, \quad (11)$$

where $c_1 \equiv \lambda S_{z,0}$, with $S_{\alpha,0}$ ($\alpha = x, y, z$) being the initial values of the components. These equations of motion for the soliton's spin can be rewritten as

$$\dot{\mathbf{S}} = \mathbf{S} \times \mathbf{B}_{\text{eff}}, \quad \mathbf{B}_{\text{eff}} = \{2\tilde{\Omega}, 0, 2\lambda^2 S_z - 2(\lambda c_1 - \delta)\}. \quad (12)$$

This represents the Bloch equations for the spin precession under the action of the effective magnetic field \mathbf{B}_{eff} . The macroscopic SOC for the soliton as a quantum body is determined by the effect of the evolution of the spin on the soliton's longitudinal momentum, resulting in a coupled nonlinear dynamics of the soliton's spin and position. At first glance, nonlinear terms in Eqs. (9)–(11) arise essentially from the SOC strength λ . However, the atomic interactions also play a fundamental role, as in the no-interaction limit, $\tilde{\Omega} = 0$, these

equations reduce to the linear Bloch precession under a fixed effective magnetic field.

To tackle solutions of the nonlinear Bloch equation, we first integrate Eq. (9), dividing it by Eq. (11). This yields $S_x = c_2 - (\lambda^2/2)\tilde{\Omega}^{-1}S_z^2 + (\lambda c_1 - \delta)\tilde{\Omega}^{-1}S_z$, where $c_2 \equiv S_{x,0} + (\delta - c_1\lambda)\tilde{\Omega}^{-1}S_{z,0} + (\lambda^2/2)\tilde{\Omega}^{-1}S_{z,0}^2$ is a constant determined by the initial conditions. Next, we focus on the case of $\delta = \lambda c_1$, which implies a particular relation between the strengths of the Zeeman splitting and SOC, making the analysis more explicit. By differentiating Eq. (11), we then arrive at a standard equation of anharmonic oscillations for the single spin component S_z ,

$$\frac{d^2 S_z}{dt^2} + \Xi S_z + 2\lambda^4 S_z^3 = 0, \quad (13)$$

where $\Xi \equiv 4\tilde{\Omega}(\tilde{\Omega} - c_2\lambda^2)$ may be positive or negative. Equation (13) has a usual solution [72]

$$S_z(t) = \frac{\sqrt{1 - \Xi\tau^2}}{2\lambda^2\tau} \text{cn}(t/\tau, k), \quad k^2 = \frac{1}{2}(1 - \Xi\tau^2), \quad (14)$$

where cn is the Jacobi's cosine with modulus k , and τ is an arbitrary parameter taking values $\tau < 1/\sqrt{|\Xi|}$. In the case of $\Xi > 0$, the linearized version of Eq. (13), which corresponds to $\tau \rightarrow 1/\sqrt{|\Xi|}$ in Eq. (14), gives rise to free Rabi oscillations with frequency $\sqrt{\Xi}$. In the general case, the frequency given by solution (14), $\omega_{\text{osc}} = \pi/[2\tau K(k)]$, where $K(k)$ is the complete elliptic integral, exceeds $\sqrt{\Xi}$ due to the nonlinear shift. Note also that the nonlinearity may give rise to oscillations in the case of $\Xi < 0$, when the free Rabi oscillations are impossible.

Further, in the spin representation, Eq. (5) can be written as $\dot{k}_+ = -2\lambda\tilde{\Omega}S_y$, which accounts for the effect of the evolution of the spin on the center-of-mass momentum. This leads to the following equation of motion for the center-of-mass

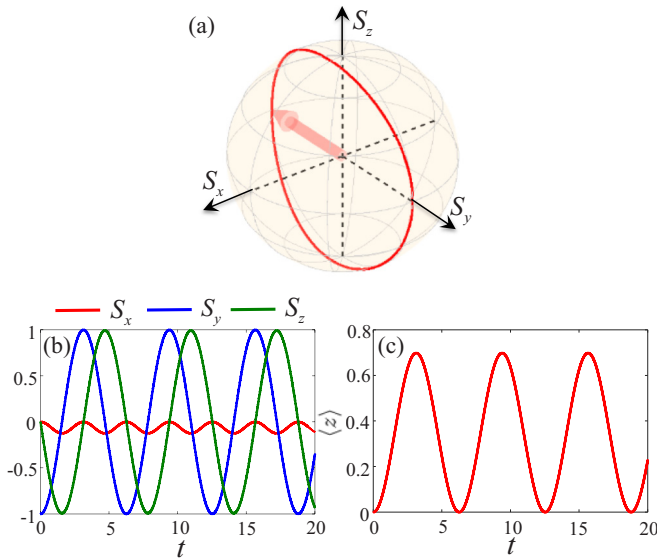


FIG. 1. The track of the spin density on the Bloch sphere (a), and the corresponding evolution of the spin components (b) and center-of-mass coordinate (c) of the soliton for the initially balanced state, with $\theta(t=0) = \pi/4$, and initial phase difference $\varphi_-(t=0) = \pi/4$ [see Eq. (3)]. Other parameters are $\Omega = 0.5$, $\lambda = 0.5\sqrt{\Omega}$, $\delta = 0$, and $g = -10$. z and t are measured in units of a_\perp and ω_\perp^{-1} .

coordinate:

$$\frac{d^2 \langle z \rangle}{dt^2} = -2\lambda\tilde{\Omega}S_y. \quad (15)$$

In other words, if we consider the soliton as a macroscopic quantum body carrying the intrinsic angular momentum, Eq. (15) represents the driving force, exerted by the intrinsic momentum and acting on the linear momentum, which is literally the macroscopic SOC. We stress that the mechanism of the soliton's motion is definitely different from the conventional collective dipole oscillations of BEC in a harmonic-oscillator trap. Indeed, in the present case the force which drives the motion of solitons under the action of SOC is the spin precession, rather than the force induced by the external potential [16,66,67]. On the other hand, here we consider an effectively mechanical motion, which is produced by the interplay of the nonlinear self-trapping and SOC.

To illustrate the soliton dynamics in detail, we display, in Fig. 1, numerical solutions of Eqs. (9)–(11) and (15), with initially balanced populations in the two components, which correspond to $\theta(t=0) = \pi/4$ and $\varphi_-(t=0) = \pi/4$. First, in Fig. 1(a) we show that the soliton spin moves along a closed orbit on the Bloch sphere. Accordingly, perfect periodic oscillations of the spin can be identified in Fig. 1(b), and perfectly periodic motion of the soliton's central coordinate is seen in Fig. 1(c). In particular, for weaker SOC, the center-of-mass oscillations can be approximated as

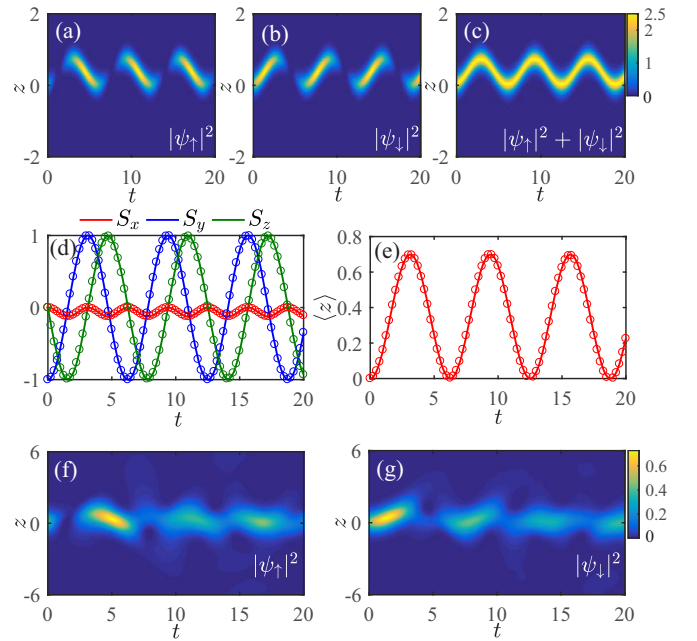


FIG. 2. (a)–(c) The evolution of the density in the two components of the soliton produced by the GP simulations for the initially balanced state with $\theta(t=0) = \pi/4$ and $\varphi_-(t=0) = \pi/4$. The parameters are $\Omega = 0.5$, $\lambda = 0.5\sqrt{\Omega}$, $\delta = 0$, and $g = -10$. The spin dynamics and center-of-mass motion of the soliton, generated by these simulations (circles), and by the variational approximation based on Eqs. (9)–(11) and (15) (solid lines), are depicted in (d) and (e). (f) and (g) display decay of the soliton in the case of a weaker atomic interaction, $g = -3$. z and t are measured in units of a_\perp and ω_\perp^{-1} .

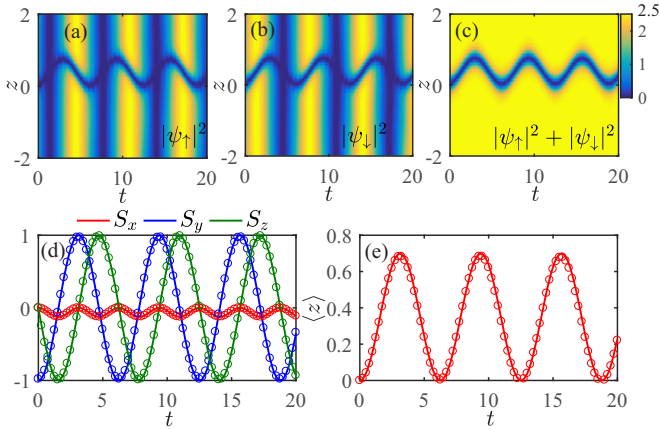


FIG. 3. (a)–(c) The same as in Fig. 2, but for the dark soliton, in the case of $g = 10$. z and t are measured in units of a_{\perp} and ω_{\perp}^{-1} .

$\langle z \rangle \simeq (\lambda/\tilde{\Omega}) \sin^2(\tilde{\Omega}t)$ with amplitude $\lambda/\tilde{\Omega}$ and a period $\pi/\tilde{\Omega}$, which depend on the strengths of SOC, Raman coupling, and atomic interaction.

To test these findings obtained in the variational (i.e., effectively mechanical) approximation, we numerically solved the GP system (1) with the input in the form of BB solitons, $\psi_{\uparrow} = \sqrt{\eta/2}(\sin\theta_0)\text{sech}(\eta z)e^{i(\lambda z + \varphi_{\uparrow,0})}$ and $\psi_{\downarrow} = \sqrt{\eta/2}(\cos\theta_0)\text{sech}(\eta z)e^{i(-\lambda z + \varphi_{\downarrow,0})}$. In Figs. 2(a)–2(c), the density of the soliton’s components exhibits remarkable periodic oscillations, and the soliton maintains its initial hyperbolic-secant profile for many oscillation cycles. Note that, although the initial momenta of the two components are opposite, the soliton does not split. In Figs. 2(d) and 2(e), we show that the direct GP simulations agree very well with the variational (mechanical) approximation. For weaker atomic interactions, the simulations show that solitons decay under the action of SOC for $\pi\lambda/\eta > (\pi\lambda/\eta)_c \approx 0.4$, as shown in Figs. 2(f) and 2(g). Furthermore, when $\delta \neq c_1\lambda$, we find that, besides the SOC-driven oscillation, the soliton would exhibit an additional linear motion, as found for the initially polarized case with $\theta(t=0) = \pi/2$ and $\delta = c_1\lambda$ (see the Supplemental Material [71] for details).

Now, we proceed to the case of the repulsive BEC nonlinearity, which is more relevant to current experiments with SOC condensates [15–18]. In this case, we introduce the following variational ansatz for dark-dark (DD) solitons:

$$\begin{pmatrix} \psi_{\uparrow} \\ \psi_{\downarrow} \end{pmatrix} = \sqrt{\frac{\eta}{2}} \begin{pmatrix} (\sin\theta) \tanh(\eta z + \xi) e^{i(k_{\uparrow}z + \varphi_{\uparrow})} \\ (\cos\theta) \tanh(\eta z + \xi) e^{i(k_{\downarrow}z + \varphi_{\downarrow})} \end{pmatrix}. \quad (16)$$

Inserting the ansatz (16) into the Lagrangian, one needs to renormalize the integrals to exclude divergent contributions of the nonvanishing background [73–77]. The analysis yields the same EL equations as Eqs. (6)–(8), but with $\eta = g/2$ for repulsive $g > 0$. We have also performed the respective direct simulations of the GP system with the initial conditions corresponding to the DD solitons, $\psi_{\uparrow} = \sqrt{\eta/2}(\sin\theta_0) \tanh(\eta z)e^{i(\lambda z + \varphi_{\uparrow,0})}$ and $\psi_{\downarrow} = \sqrt{\eta/2}(\cos\theta_0) \tanh(\eta z)e^{i(-\lambda z + \varphi_{\downarrow,0})}$. The results are depicted in Fig. 3, where the DD soliton displays oscillations similar to those reported above for the BB configuration. Note that the two components of the background alternately disappear and revive, as shown in Figs. 3(a) and 3(b).

In experiments, the condensate is usually trapped in a harmonic-oscillator potential, $V(z) = \gamma^2 z^2/2$, which affects the motion of solitons [60–65]. In this case, the EL equations for variational parameters k_{\pm} and ξ are modified to $\dot{k}_{\pm} = -2\lambda\tilde{\Omega}S_{\pm} + (\gamma^2/\eta)\xi$ and $\dot{\xi} = -k_{\pm}\eta$, with η satisfying the condition $4\eta^4 + 2g\eta^3 = \pi^2\gamma^2$. Correspondingly, the center-of-mass motion would acquire an additional trap-dependent term $\frac{d^2\langle z \rangle}{dt^2} + \gamma^2\langle z \rangle = -2\lambda\tilde{\Omega}S_y$, which gives rise to an additional collective oscillation with a period $\simeq 2\pi/\gamma$, as shown in Fig. 4. For a weak trap, the period of trap-driven oscillation and the characteristic length of the trap are much larger than the period and amplitude of the SOC-driven oscillation, respectively. Hence, the SOC-driven oscillation of the soliton is not affected conspicuously by a weak trap and should be distinguishable in experiment. Here, we have used a bright soliton to illustrate the effect of a (weak) axial trap. Similar results are also identified numerically for a dark soliton in a harmonic trap.

Finally, we discuss some related experimental issues. So far, the Raman-induced SOC has been realized for the BEC in the ^{87}Rb gas with repulsive atomic interactions. We assume an elongated condensate of $\sim 10^4$ atoms is trapped in a weak harmonic trap with frequencies $\omega_{\perp} = 2\pi \times 85$ Hz and $\omega_z = 2\pi \times 5.9$ Hz [65], and the corresponding ratio of the scattering lengths is $a_{\uparrow\uparrow} : a_{\uparrow\downarrow} : a_{\downarrow\downarrow} = 1 : 1 : 1.005$ [15]. In this case, at the center of the trap, we first create the stationary dark-dark solitons with width $\sim 0.5 \mu\text{m}$ by means of phase- and density-engineering techniques [12]. Then two 804.1 nm Raman lasers with an intersection angle 20° are used to create a weak SOC. With the above parameters, the period and amplitude of SOC-driven oscillation of solitons are about 11 ms and $2 \mu\text{m}$, respectively, which may be further adjusted by varying the SOC, Raman coupling, and atomic interaction. These results show that the SOC-driven oscillations can be experimentally observed.

In summary, we have shown that the interplay of the SOC (spin-orbit coupling), Raman coupling, and intrinsic nonlinearity in quasi-1D BEC may realize the mechanism of SOC in the form of a mechanical motion of bright and dark solitons, considered as macroscopic quantum bodies. The soliton’s angular momentum (spin) evolves according to

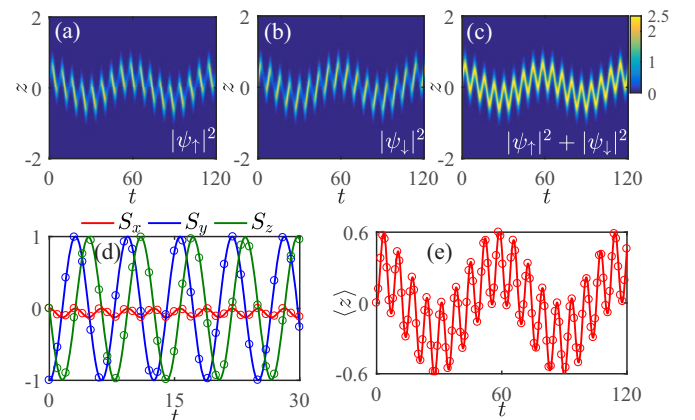


FIG. 4. The results for bright-bright solitons in the trap with $\gamma = 0.1$, the other parameters are the same as in Fig. 2. z and t are measured in units of a_{\perp} and ω_{\perp}^{-1} .

the Bloch equation under the action of an effective magnetic field, and induces a force affecting the motion of the soliton's central coordinate. The results have been obtained by means of a variational analysis and numerical simulations, which demonstrate very good agreement. These findings suggest directions for experimental studies of the motion of matter-wave solitons under the action of SOC.

We thank Hui Zhai and U. Zuelicke for valuable discussions. This work is supported by NSFC under Grants

No. 11474205, No. 11404225, and No. 11504037. L.W. is also supported by the Chongqing Research Program of Basic Research and Frontier Technology under Grant No. cstc2015jcyjA50024, and the Foundation of Education Committees of Chongqing under Grant No. KJ1500311. The work of B.A.M. is supported, in part, by the joint program in physics between the National Science Foundation (U.S.) and Binational Science Foundation (U.S.-Israel), through Grant No. 2015616. G.J. was supported by the Lithuanian Research Council (Grant No. MIP-086/2015).

-
- [1] K. E. Strecker, G. B. Partridge, A. G. Truscott, and R. G. Hulet, *New J. Phys.* **5**, 73 (2003).
- [2] V. A. Brazhnyi and V. V. Konotop, *Mod. Phys. Lett. B* **18**, 627 (2004).
- [3] F. Kh. Abdullaev, A. Gammal, A. M. Kamchatnov, and L. Tomio, *Int. J. Mod. Phys. B* **19**, 3415 (2005).
- [4] O. Morsch and M. Oberthaler, *Rev. Mod. Phys.* **78**, 179 (2006).
- [5] B. A. Malomed, *Soliton Management in Periodic Systems* (Springer, Berlin, 2006).
- [6] G. Juzeliūnas, J. Ruseckas, P. Öhberg, and M. Fleischhauer, *Lithuanian J. Phys.* **47**, 351 (2007).
- [7] P. G. Kevrekidis, D. J. Frantzeskakis, and R. Carretero-González, *Emergent Nonlinear Phenomena in Bose-Einstein Condensates* (Springer, Berlin, 2008).
- [8] Y. V. Kartashov, B. A. Malomed, and L. Torner, *Rev. Mod. Phys.* **83**, 247 (2011).
- [9] P. G. Kevrekidis and D. J. Frantzeskakis, [arXiv:1512.06754](https://arxiv.org/abs/1512.06754).
- [10] S. Burger, K. Bongs, S. Dettmer, W. Ertmer, K. Sengstock, A. Sanpera, G. V. Shlyapnikov, and M. Lewenstein, *Phys. Rev. Lett.* **83**, 5198 (1999).
- [11] L. Khaykovich, F. Schreck, G. Ferrari, T. Bourdel, J. Cubizolles, L. D. Carr, Y. Castin, and C. Salomon, *Science* **296**, 1290 (2002).
- [12] K. E. Strecker, G. B. Partridge, A. G. Truscott, and R. G. Hulet, *Nature (London)* **417**, 150 (2002).
- [13] S. L. Cornish, S. T. Thompson, and C. E. Wieman, *Phys. Rev. Lett.* **96**, 170401 (2006); A. L. Marchant, T. P. Billam, T. P. Wiles, M. M. H. Yu, S. Gardiner, and S. L. Cornish, *Nat. Commun.* **4**, 1865 (2013).
- [14] J. H. V. Nguyen, P. Dyke, D. Luo, B. A. Malomed, and R. G. Hulet, *Nat. Phys.* **10**, 918 (2014).
- [15] Y.-J. Lin, K. Jiménez-García, and I. B. Spielman, *Nature (London)* **471**, 83 (2011).
- [16] J.-Y. Zhang, S.-C. Ji, Z. Chen, L. Zhang, Z.-D. Du, B. Yan, G.-S. Pan, B. Zhao, Y.-J. Deng, H. Zhai, S. Chen, and J.-W. Pan, *Phys. Rev. Lett.* **109**, 115301 (2012).
- [17] P. J. Wang, Z.-Q. Yu, Z. K. Fu, J. Miao, L. H. Huang, S. J. Chai, H. Zhai, and J. Zhang, *Phys. Rev. Lett.* **109**, 095301 (2012).
- [18] L. W. Cheuk, A. T. Sommer, Z. Hadzibabic, T. Yefsah, W. S. Bakr, and M. W. Zwierlein, *Phys. Rev. Lett.* **109**, 095302 (2012).
- [19] C. J. Wang, C. Gao, C.-M. Jian, and H. Zhai, *Phys. Rev. Lett.* **105**, 160403 (2010); H. Zhai, *Int. J. Mod. Phys. B* **26**, 1230001 (2012).
- [20] T.-L. Ho and S. Z. Zhang, *Phys. Rev. Lett.* **107**, 150403 (2011).
- [21] Z. F. Xu, R. Lü, and L. You, *Phys. Rev. A* **83**, 053602 (2011).
- [22] Y. P. Zhang, L. Mao, and C. W. Zhang, *Phys. Rev. Lett.* **108**, 035302 (2012).
- [23] Y. Li, L. P. Pitaevskii, and S. Stringari, *Phys. Rev. Lett.* **108**, 225301 (2012).
- [24] J. P. Vyasanakere, S. Zhang, and V. B. Shenoy, *Phys. Rev. B* **84**, 014512 (2011).
- [25] H. Hu, L. Jiang, X.-J. Liu, and H. Pu, *Phys. Rev. Lett.* **107**, 195304 (2011).
- [26] M. Gong, S. Tewari, and C. W. Zhang, *Phys. Rev. Lett.* **107**, 195303 (2011).
- [27] Z.-Q. Yu and H. Zhai, *Phys. Rev. Lett.* **107**, 195305 (2011).
- [28] M. Gong, G. Chen, S.-T. Jia, and C. W. Zhang, *Phys. Rev. Lett.* **109**, 105302 (2012).
- [29] C.-L. Qu, Z. Zheng, M. Gong, Y. Xu, L. Mao, X. Zou, G. Guo, and C. Zhang, *Nat. Commun.* **4**, 2710 (2013).
- [30] W. Zhang and W. Yi, *Nat. Commun.* **4**, 2711 (2013).
- [31] V. Galitski and I. B. Spielman, *Nature (London)* **494**, 49 (2013).
- [32] N. Goldman, G. Juzeliūnas, P. Öhberg, and I. B. Spielman, *Rep. Prog. Phys.* **77**, 126401 (2014).
- [33] H. Zhai, *Rep. Prog. Phys.* **78**, 026001 (2014).
- [34] S.-W. Su, S.-C. Gou, Q. Sun, L. Wen, W.-M. Liu, A.-C. Ji, J. Ruseckas, and G. Juzeliūnas, *Phys. Rev. A* **93**, 053630 (2016).
- [35] Y. Xu, Y. Zhang, and B. Wu, *Phys. Rev. A* **87**, 013614 (2013).
- [36] Y. V. Kartashov, V. V. Konotop, and F. K. Abdullaev, *Phys. Rev. Lett.* **111**, 060402 (2013).
- [37] V. Achilleos, J. Stockhofe, P. G. Kevrekidis, D. J. Frantzeskakis, and P. Schmelcher, *Europhys. Lett.* **103**, 20002 (2013).
- [38] V. Achilleos, D. J. Frantzeskakis, P. G. Kevrekidis, and D. E. Pelinovsky, *Phys. Rev. Lett.* **110**, 264101 (2013).
- [39] Y. K. Liu and S. J. Yang, *Europhys. Lett.* **108**, 30004 (2014).
- [40] Y. V. Kartashov, V. V. Konotop, and D. A. Zezyulin, *Phys. Rev. A* **90**, 063621 (2014).
- [41] S. Gautam and S. K. Adhikari, *Laser Phys. Lett.* **12**, 045501 (2015).
- [42] S. Gautam and S. K. Adhikari, *Phys. Rev. A* **91**, 063617 (2015).
- [43] Y. Zhang, Y. Xu, and T. Busch, *Phys. Rev. A* **91**, 043629 (2015).
- [44] V. Achilleos, D. J. Frantzeskakis, and P. G. Kevrekidis, *Phys. Rev. A* **89**, 033636 (2014).
- [45] S. Peotta, F. Mireles, and M. Di Ventra, *Phys. Rev. A* **91**, 021601(R) (2015).
- [46] H. Sakaguchi, B. Li, and B. A. Malomed, *Phys. Rev. E* **89**, 032920 (2014); H. Sakaguchi, E. Ya. Sherman, and B. A. Malomed, *ibid.* **94**, 032202 (2016); H. Sakaguchi and B. A. Malomed, *New J. Phys.* **18**, 025020 (2016).
- [47] L. Salasnich, W. B. Cardoso, and B. A. Malomed, *Phys. Rev. A* **90**, 033629 (2014).

- [48] H. Sakaguchi and B. A. Malomed, *Phys. Rev. E* **90**, 062922 (2014).
- [49] V. E. Lobanov, Y. V. Kartashov, and V. V. Konotop, *Phys. Rev. Lett.* **112**, 180403 (2014).
- [50] P. Beličev, G. Gligorić, J. Petrović, A. Maluckov, L. Hadzievski, and B. Malomed, *J. Phys. B* **48**, 065301 (2015).
- [51] Y.-C. Zhang, Z.-W. Zhou, B. A. Malomed, and H. Pu, *Phys. Rev. Lett.* **115**, 253902 (2015).
- [52] O. Fialko, J. Brand, and U. Zulicke, *Phys. Rev. A* **85**, 051605(R) (2012).
- [53] Y. S. Kivshar and B. A. Malomed, *Rev. Mod. Phys.* **61**, 763 (1989).
- [54] Yu. S. Kivshar and D. E. Pelinovsky, *Phys. Rep.* **331**, 117 (2000).
- [55] Y. S. Kivshar and G. P. Agrawal, *Optical Solitons: From Fibers to Photonic Crystals* (Academic, San Diego, 2003).
- [56] B. A. Malomed, D. Mihalache, F. Wise, and L. Torner, *J. Opt. B* **7**, R53 (2005).
- [57] A. S. Desyatnikov, L. Torner, and Y. S. Kivshar, *Prog. Opt.* **47**, 1 (2005).
- [58] D. Mihalache, *Rom. J. Phys.* **57**, 352 (2012).
- [59] V. V. Konotop, J. Yang, and D. A. Zezyulin, *Rev. Mod. Phys.* **88**, 035002 (2016).
- [60] T. Busch and J. R. Anglin, *Phys. Rev. Lett.* **84**, 2298 (2000); **87**, 010401 (2001).
- [61] L. D. Carr and Y. Castin, *Phys. Rev. A* **66**, 063602 (2002); L. Salasnich, *ibid.* **70**, 053617 (2004); Z. X. Liang, Z. D. Zhang, and W. M. Liu, *Phys. Rev. Lett.* **94**, 050402 (2005).
- [62] L. Li, B. A. Malomed, D. Mihalache, and W. M. Liu, *Phys. Rev. E* **73**, 066610 (2006).
- [63] A. Weller, J. P. Ronzheimer, C. Gross, J. Esteve, M. K. Oberthaler, D. J. Frantzeskakis, G. Theocharis, and P. G. Kevrekidis, *Phys. Rev. Lett.* **101**, 130401 (2008).
- [64] X. X. Liu, H. Pu, B. Xiong, W. M. Liu, and J. Gong, *Phys. Rev. A* **79**, 013423 (2009).
- [65] C. Becker, S. Stellmer, P. Soltan-Panahi, S. Dörscher, M. Baumert, E.-M. Richter, J. Kronjäger, K. Bongs, and K. Sengstock, *Nat. Phys.* **4**, 496 (2008).
- [66] Z. Chen and H. Zhai, *Phys. Rev. A* **86**, 041604 (2012).
- [67] Y. Li, G. I. Martone, and S. Stringari, *Europhys. Lett.* **99**, 56008 (2012).
- [68] S. V. Manakov, *Zh. Eksp. Teor. Fiz.* **65**, 505 (1974) [*Sov. Phys. JETP* **38**, 248 (1974)].
- [69] B. A. Malomed, *Prog. Opt.* **43**, 71 (2002).
- [70] R. Navarro, R. Carretero-González, and P. G. Kevrekidis, *Phys. Rev. A* **80**, 023613 (2009); L. Wen, W. M. Liu, Y. Cai, J. M. Zhang, and J. Hu, *ibid.* **85**, 043602 (2012).
- [71] See Supplemental Material at <http://link.aps.org/supplemental/10.1103/PhysRevA.94.061602> for the derivation of the Euler-Lagrange equations, and additional simulations of the soliton dynamics.
- [72] I. S. Gradshteyn and I. M. Ryzhik, *Tables of Integrals, Series, and Products*, 7th ed. (Elsevier, Amsterdam, 2007).
- [73] I. V. Barashenkov and A. O. Harin, *Phys. Rev. Lett.* **72**, 1575 (1994).
- [74] R. Carretero-González, D. J. Frantzeskakis, and P. G. Kevrekidis, *Nonlinearity* **21**, R139 (2008).
- [75] D. J. Frantzeskakis, *J. Phys. A* **43**, 213001 (2010).
- [76] Y. S. Kivshar and X. Yang, *Phys. Rev. E* **49**, 1657 (1994).
- [77] I. M. Uzunov and V. S. Gerdjikov, *Phys. Rev. A* **47**, 1582 (1993).